LAWRENCE
LIVERMORE
NATIONAL
LABORATORY

LLNL-JRNL-431771

An imaging proton spectrometer for short-pulse laser plasma experiments

H. Chen, A. Hazi, R. van Maren, S. Chen, J. Fuchs, M. Gauthier, S. Le Pape, J. R. Rygg, R. Shepherd

May 13, 2010

Review Sceientific Instruments

Disclaimer

An imaging proton spectrometer for short-pulse laser plasma experiments [a)]

Hui Chen[1, b)], A. Hazi[1], R. van Maren[1], S. Chen[1], J. Fuchs[2], M. Gauthier[2], S. Le Pape[1], J. R. Rygg[1], R. Shepherd[1]

[1] *Lawrence Livermore National Laboratory,Livemore, CA 94551, USA*
[2] *LULI Ecole Polytechnique, 91128 Palaiseau Cedex, France*

(Presented XXXXX; received XXXXX; accepted XXXXX; published online XXXXX)
(Dates appearing here are provided by the Editorial Office)

Ultra intense short pulse laser pulses incident on solid targets can generate energetic protons. In additions to their potentially important applications such as in cancer treatments and proton fast ignition, these protons are essential to understand the complex physics of intense laser plasma interaction. To better characterize these laser-produced protons, we designed and constructed a novel, spatially imaging proton spectrometer that will not only measure proton energy distribution with high resolution, but also provide its angular characteristics. The information obtained from this spectrometer compliments those from commonly used diagnostics including radiochromic film packs, CR39 nuclear track detectors, and non-imaging magnetic spectrometers. The basic characterizations and sample data from this instrument are presented.

I. Introduction

Since the discovery on the NOVA laser in 1998 [1] that intense short pulse lasers can accelerate proton beams with multi-MeV energies, a great deal of research has been performed to understand the process of laser-driven ion acceleration and various potential applications of the resulting ion beams [2]. This includes efforts to characterize the physics of acceleration, beam quality, laser to proton conversion efficiency, and maximum proton energy scaling with laser parameters. Majority of the previous research has focused on the high-energy (> few MeV) protons. This is partly because higher energy protons are more relevant the applications such as proton fast ignition research [3] and proton radiography of dense matter [4], and partly due to the use of radiochromic film (RCF) packs, which are insensitive to low energy protons, to measure their energy and angular distributions. The measurement and understanding of laser accelerated, low-energy (<few MeV) protons are particularly important due to the fact these porotons can efficiently heat (isochorically) solid samples to the 'warm dense matter' regime. In addition, there is a great need for experimental verification of ion energy loss physics in plasma modeling codes, particularly in the moderately-strongly coupled regime [5]. Low-energy proton beams offer a good tool to address this need, as the stopping at low energies is more sensitive to the ion-plasma interaction physics. To help answer these fundemental questions in the field of high energy density physics, we designed and constructed a high energy-resolution, imaging proton spectrometer (IPS) that covers the 0.05 – 5 MeV energy range. This paper describes the design principles and modeling analysis, as well as sample results from a laser-solid interaction experiment.

II. Spectrometer description

The design of the imaging proton spectrometer (IPS) is based on the fact that the laser accelerated protons are ballistic and behave as if they were emitted from a virtual point source [2]. Consequently, one may in principle trace their trajectories back to their origin (source), as illustrated in Fig. 1. The energy dispersion of the IPS is achieved by a pair of permanent magnets. Charged particles in the magnetic field will move along a curved trajectory (perpendicular to the field) with a Larmour radius determined by their kinetic energy and the charge to mass ratio. In the present design, the protons are detected near the side-wall of the spectrometer, in contrast to previous implementations, where they are detected at the back wall facing the entrance apperture [6].

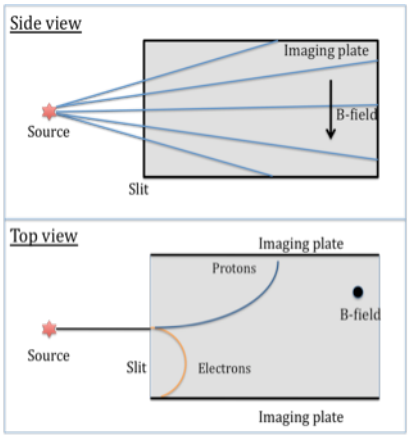

FIG 1: The schmatic of the IPS. *Top (side view)*: the imaging property based on straight trajectories of the protons in the xy-plane. *Bottom (top view)*; the energy dispersion of the IPS.

In principle, the IPS can be used to measure the energy spectrum of fast electrons as well. However, electron measurement is only secondary in the present instrument since the magnctic field strength was chosen to optimize the proton measurement. The actual imaging and dispersion properties of the IPS are not simple due to the magnetic structure of the spectrometer, as will be discussed below. The energy coverage of the spectrometer is between 50 keV to ~5 MeV. We chose photostimulable image plates (IPs) as the proton detector, since

[a)]Contributed paper published as part of the Proceedings of the 18th Topical Conference on High-Temperature Plasma Diagnostics, Wildwood, New Jersey, May, 2010.
[b)]Author to whom correspondence should be addressed. Electonic mail: chen33@llnl.gov

they can provide a large dynamic range [7] and high sensitivity to energetic (> 100 keV) protons. The spectrometer is designed to be compact with approximate dimensions of 13 cm x 8.5 cm x 19 cm. This is particularly important because usually only limited amount of space is available for an individual diagnostic in vacuum chambers used in intense laser-solid interaction experiments. To cut down the background noise from high energy photons, the whole spectrometer is shielded in the front with "heavy" metal in combination with low Z plastic. The body is fabricated from 0.5 inch-thick steel.

A. Energy dispersion

The dispersion (proton energy vs. position on the image plate detector) of the spectrometer was determined using a combination of measurements and simulations of the magnetic field inside the instrument. A Faraday probe was used to map the y-component of the magnetic field (the component parallel to the slit) as a function of position in a plane defined by the slit and the long-axis of the spectrometer. For these measurements, the slit assembly was removed, and the probe was inserted through a slot in the front steel plate. The accuracy of the field mapping was limited by the flexing of the thin arm holding the probe at long extensions beyond the front plate. Simulations of the magnetic field were performed using the 2D finite-element magnetic code FEMM (v4.2) [8]. For these calculations, the dimensions of the critical components of the spectrometer were imported directly from the CAD drawing of the entire instrument. The magnetic properties of the various components were taken from the built-in materials library in FEMM. The 2D mesh was chosen sufficiently dense (~60K nodes and ~115K elements) and so that the calculated B-field values were stable within a few percent.

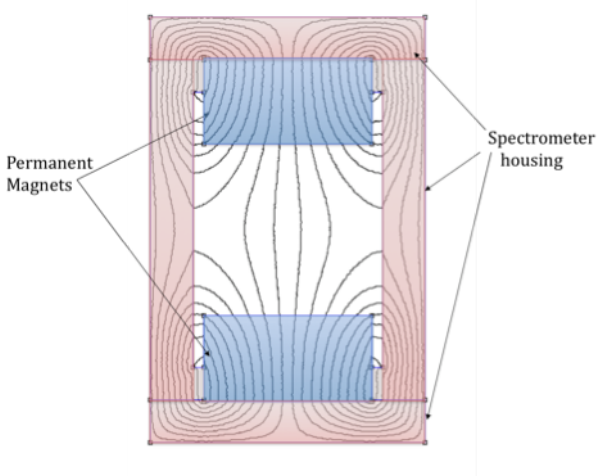

FIG 2. The magnetic structure of the IPS (front view) modeled by the FEMM code. The magnetic field is not uniform; the closer it is to the magnets, the stronger is the magnetic field.

Because of the relatively large separation of the magnets required for spatial imaging, there is significant spatial variation of the magnetic field, with B_y increasing by approximately a factor of 2 from mid-way between the magnets to locations adjacent to the magnets, as shown in Fig. 2. Along the direction perpendicular to the slit (z-axis), B_y approaches zero at the side walls of the spectrometer. The dispersion along the center-line of the image plate was determined semi-analytically using the calculated values of $B_y(z)$ and the distance between the slit and the image plate. The absolute value of the magnetic field (and the dispersion at a single energy) was calibrated by measuring the proton spectrum with an image plate (Fuji Photo Film Ltd., type BAS-MS-2040), which has a 9 μm PET layer on the top of the active layer [7]. The PET layer acts as a range-filter and results in a sharp, low-energy cut-off in the spectrum [9]. We used the stopping power of PET [10], along with the calculated angle of incidence of the protons on the image plate at the spatial location of the cut-off, to determine the proton energy corresponding to that location. The energy resolving power (E/dE) of the IPS is about 250 at 0.5 MeV and ~350 at 2 MeV. This is substantially higher than that can be achieved with RCF pack.

The dispersion at all points on the image plane can be constructed using a 3D code. However, it can also be derived experimentally. Shown below is the image of a measured spectrum, superimposed with the fitted 2D dispersion contours, where the dispersion along the center line is constrained by the calibrated, analytical dispersion curve discussed above.

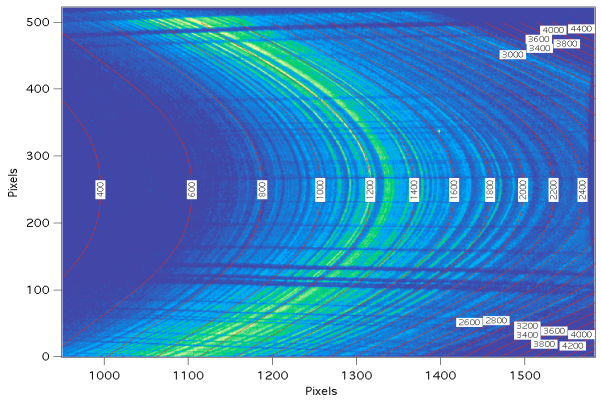

FIG 3: The iso-energy contours of the IPS dispersion superimposed on a measured spectum. The numbers listed are the energy in the unit of keV. The image is about 5 cm wide and 15 cm long. The pixel size is 100 μm x100 μm.

B. Imaging property

The imaging capability of the spectrometer is achieved by using a long (~5 cm), narrow slit, parallel to the magnetic field, through which the protons enter the interior of the instrument. The width of the slit (w_s) is adjustable and is normally set between 50 and 100 μm to maintain good energy resolution. The narrow slit geometrically constrains the position and velocity of the entrant protons in the z-direction, perpendicular to the slit. Therefore, one needs to consider only the proton's entry point along the slit (y_s) and its two velocity components (v_x and v_v). For a diverging laminar beam emanating from a point source, y_s is determined by the geometrical relation: $(y_s - y_0)/L = v_v/v_x$, where y_0 is the vertical position of the source point relative to the centerline of the IPS and L is the distance (along x) between the source and the slit. L and y_0 are the same for all protons in the beam regardless of their angle of incidence. This allows one to reconstruct the energy and angle of the incident proton from its

landing position (x,y) on the image plate detector. In the direction perpendicular to the slit, the field of view of the IPS is ~2 mm, for L=12 cm and w_s=100 μm (typical values). In the direction parallel to the slit, the acceptance angle of the IPS is about ± 5 degrees, assuming $y_0 \approx 0$ and L=12 cm.

III. Test of the IPS in a laser experiment

We tested the imaging property as well as the energy dispersion characteristic of the IPS on the Titan laser at the Jupiter Laser Facility at the Lawrence Livermore National Laboratory [11]. Fig. 4 shows the experimental setup and a sample result illustrating the imaging capability of the IPS. Several carbon foils (with various thickness and widths) were mounted across the slit of the IPS at different positions. These foils served as fiducial markers by creating shadows on the image plate by stopping protons coming from the source at certain angles. In this experiment, two separate laser pulses from Titan illuminated two different targets creating two spatially separated proton sources (A and B). Source A was made by irradiating a 10-μm thick Al foil with 73 J laser energy in 10 ps, with a 10 μm diameter focal spot. The laser intensity was about $5x10^{18}$ Wcm^{-2} corresponding to maximum proton energy of 1-2 MeV [12], as shown in Fig. 4. The second source (B) was made by a lower intensity but higher energy laser pulse (170 J, 10 ps with 300 μm diameter focal spot, equivalent to $1x10^{16}$ Wcm^{-2}) irradiating a 10-μm thick vanadium target. The measured maximum proton energy for source B is about 300 keV. The spacing of the two sources was about 350 μm, and is well resolved by the IPS, as shown in Fig. 4.

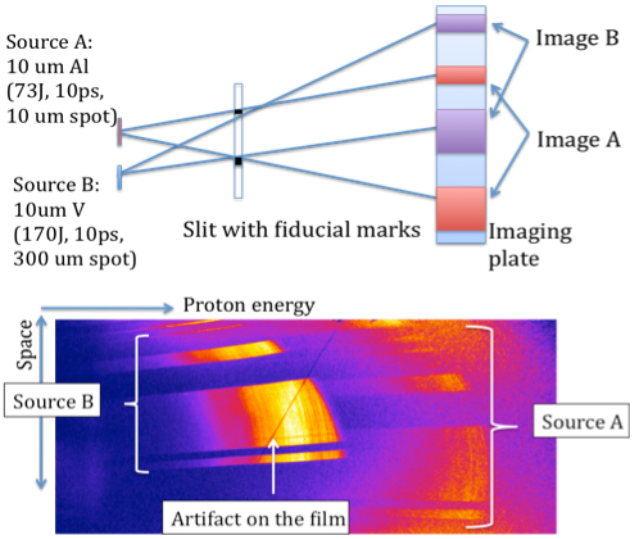

FIG 4. The schematics of the experimental setup (top) and the resulting spatially resolved proton image (bottom). The laser and target condition for the two sources are noted. Two proton sources are clearly imaged on the energy dispersing image plane, with the dark gaps being caused by the C-foils mounted across the slit. The thin slanted line on the image is caused by a artifact (scratch) on the imge plate and is not related to the proton sources.

Fig. 5 shows a sample proton energy spectrum obtained with the IPS in a different experiment. The spectrum has its maximum near a proton energy of 100 keV, and then decreases quasi-exponentially at higher energies [2]. The physics behind the structure in the measured spectrum is to be studied in the future.

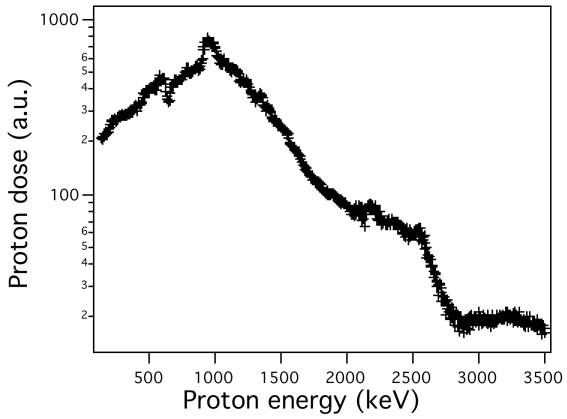

FIG 5. Sample proton energy spectrum taken by the IPS from a short-pulse laser experiment.

IV. Summary and future work

In this paper we describe the design and test of a new imaging proton spectrometer. This instrument features physical compactness, high resolving power for the proton energy and the ability to image the proton source. We expect it will be useful in measuring the source structure and energy spectrum of low energy (< few MeV) protons produced in short pulse laser-solid interaction experiments. Future work on the IPS will include absolute calibration of the image plate((IP) detection system in the current geometry, so that the measured IP counts per pixel can be converted to number of protons. Calibration of the energy dispersion at multiple energies is also desirable to improve the accuracy of the present dispersion curve based on simulations and measurement with a range-filter at a single energy.

This work was performed under the auspices of the U.S. Department of Energy by Lawrence Livermore National Laboratory under Contract DE-AC52-07NA27344, as part of the Cimarron project funded by LDRD-09SI11.

V. References

[1] R. A. Snavely et al., *Phys. Rev. Lett.,* **85**, 2945 (2000).
[2] For a comprehensive review, see M. Borghesi, J Fuchs, et al. *Fusion Sci. & Tech.* , **49**, 412 (2006).
[3] M. Roth et al., *Phys. Rev. Lett.,* **86**, 436 (2001); M. Temporal et al., *Phys. Plasmas*, **9**, 3098 (2002).
[4] See Section IV.A in Ref. 2.
[5] V Fortov et al., *Physics of Strongly Coupled Plasma,* Oxford University Press, U.S., 2006.
[6] A. Mancic et al., *Rev. Sci. Instr.* **79**, 073301 (2008).
[7] http://www.fujifilm.com/products/life_science/si_imgplate/whatis02.html; http://fujifilmlifescienceusa.com/imaging.htm.
[8] http://femm.foster-miller.com; dmeeker@ieee.org.
[9] M. P. Antici, PhD Thesis, Ecole Polytechnique, France, June 2007, Sec.A5.1
[10] SRIM-2008; J.F. Ziegler, J.P. Biersack, U. Littmark, *The Stopping and Range of Ions in Solids*, Pergamon, New York, 1985.
[11] https://jlf.llnl.gov.
[12] See Fig. 9 in Ref. 2.